Electric Power Systems Research 189 (2020) 106594

Contents lists available at ScienceDirect

Electric Power Systems Research

journal homepage: www.elsevier.com/locate/epsr

An investigation of harmonic induced voltages on medium-voltage cable sheaths and nearby pipelines

T.A. Papadopoulos[a,*], I.P. Chaleplidis[a], A.I. Chrysochos[b], G.K. Papagiannis[c], K. Pavlou[b]

[a] Department of Electrical and Computer Engineering, Democritus University of Thrace, Xanthi 67100, Greece
[b] R&D Department, Hellenic Cables, Athens 15125, Greece
[c] School of Electrical and Computer Engineering, Aristotle University of Thessaloniki, Thessaloniki 54124, Greece

ARTICLE INFO

Keywords:
Cable sheaths
Electromagnetic interference
Harmonics
Induced voltages
Pipelines

ABSTRACT

This paper investigates the impact of harmonics in underground medium-voltage cables to the induced voltages on the cable sheaths of the excited system as well as the corresponding electromagnetic interference (EMI) to nearby coated pipelines. To evaluate systematically the harmonic induced voltages on both cable sheaths and pipelines a benchmarking analysis is carried out. The accuracy of different simulation models is also investigated. The feasibility and practical application of this paper is examined in a cable system excited by current harmonics using data obtained from measurements of the recent literature.

1. Introduction

The increased installation of switching power electronic converters in power systems has raised the scientific interest in harmonic pollution problems [1]. Harmonics cause a series of issues, such as additional conductor and equipment losses, overloading of reactive power compensation capacitors, malfunction of circuit breakers, errors in electric power and energy measurements, and induced voltages to nearby metallic parts [1,2].

Specifically, harmonics flowing in underground transmission and distribution systems may cause, additional to the 50 Hz/60 Hz (fundamental frequency) current, ohmic losses and possible hazardous overvoltages in cable sheaths, as well as electromagnetic interference (EMI) to nearby metallic parts, e.g., pipelines. Both of the above issues have been thoroughly investigated in the literature, regarding induced voltages at the fundamental frequency [3-8], whereas only recently harmonic voltage induction has attracted the scientific interest. Harmonic voltage induction due to the electromagnetic coupling of parallel overhead transmission lines was first referred in [9]. Similar investigations were also carried out in [10], regarding the coupling of voltages and currents on voltage-source converter (VSC)-HVDC overhead transmission lines from neighboring a.c. lines. Induced harmonic voltages on buried pipelines caused by transmission or distribution lines have been analyzed in [2], through field measurements [11] and circuit-model analysis. More specifically, EMI issues on pipelines due to harmonics from a.c. electrified traction systems was holistically assessed in [12].

Additionally, the rapid development of renewable energy sources (RES) in power systems has increased the scientific interest on EMI issues, since such problems may exist in areas of large photovoltaic parks or wind-parks to the grid, where gas, oil or irrigation metallic pipelines may be present [8]. In most of these cases, underground cables are used for the internal network and/or the connection of the RES installations to the grid. There are only few works presenting preliminary EMI results caused by underground cables to nearby pipelines, but only regarding the fundamental frequency, while there are no similar works about harmonic induction effects. In fact, current harmonics may cause increased voltages, since induced voltages increase with frequency, according to Faraday's law and the zero-sequence pattern of the triplen currents; triplens are harmonics of odd multiples of three, e.g., 3rd, 9th, 15th, etc.

This paper investigates, for the first time according to the authors' knowledge, the impact of harmonic voltage induction in underground cable systems of distribution networks. The work focuses on the induced voltages and currents on cable sheaths and nearby coated pipelines, the latter being located in the vicinity of the excited cable system. To systematically evaluate EMI due to the presence of harmonics, a benchmarking analysis is carried out. Using this benchmark, the accuracy of different simulation models is investigated. The feasibility of this research is examined in a cable system excited by current

* Corresponding author.
E-mail addresses: thpapad@ee.duth.gr (T.A. Papadopoulos), iordchal@ee.duth.gr (I.P. Chaleplidis), achrysochos@hellenic-cables.com (A.I. Chrysochos), grigoris@eng.auth.gr (G.K. Papagiannis), kpavlou@hellenic-cables.com (K. Pavlou).

https://doi.org/10.1016/j.epsr.2020.106594
Received 11 February 2020; Received in revised form 30 June 2020; Accepted 25 July 2020
Available online 03 August 2020
0378-7796/

harmonics using data obtained from measurements of the recent literature [2].

2. Problem assumptions

In general, there are three types of EMI, named as inductive (or electromagnetic) coupling, capacitive (or electrostatic) coupling, and conductive (or resistive) coupling [4-7]. In detail:

- The calculation of inductive coupling is the most investigated mechanism. Regarding power cables, the nominal and the equivalent pi models (exact) are used, while specifically for pipeline arrangements analytical formulations and numerical simulations have been proposed.
- Capacitive coupling is mainly examined in cases of cables and pipelines located above the ground. In the case of underground systems, e.g., pipelines, capacitive coupling is negligible at low frequencies, since earth behaves as a perfect conductor [14]. Therefore, regarding power cables, capacitive coupling is considered only by means of the insulation between the cable conductor and sheath.
- Conductive coupling refers to buried metallic conductors exposed to voltage stress when earth potential rise (EPR) with respect to remote earth occurs, due to a flow of current though the surrounding soil (earth-return currents) [4]. Such cases typically refer to pole-to-ground faults; thus, conductive coupling is not considered in the current analysis.

In this study, the impact of inductive coupling and circulating currents in cables is considered for the calculation of harmonic voltages on cable sheaths and nearby pipelines.

3. Cable types and configurations

Two typical primary distribution medium-voltage (MV) underground cable arrangements are examined, namely the touching trefoil and the spaced horizontal (flat) formation, as shown in Fig. 1 [15]. In both arrangements, the cable system consists of a group of three identical MV single-core (SC) cables of 25 kV, 95 mm^2 with copper conductor, TRXLPE main insulation, concentric neutral of copper wires and LLDPE jacket. The cable geometrical and electrical properties are adjusted to model the cable parameters accurately. Initially, the stranded conductor and sheaths are considered as solid and tubular conductors, respectively, assuming the same per-unit-length d.c. resistance; thus, the original resistivity values are modified according to the formulation proposed in [16]. Next, the effect of the temperature on the resistance of the metallic parts is taken into account; the conductor and sheath modified resistivities are adjusted at 90 °C and 80 °C, according to the maximum permissible temperature of the cable insulation and jacket, respectively. Finally, the SC cable semi-conductive layers are included in the cable insulation, assuming the same per-unit-length capacitance; the thickness of the insulation is expanded and the relative permittivity is increased [16]. The adjusted properties of the MV cable system are given in Table 1. The cables are laid in a 1.0 m depth ditch and the cable spacing for the horizontal arrangement is $s = 0.15$ m. In Fig. 1, the reference of horizontal position ($y = 0$ m) for the two arrangements is depicted as well as the cable phases. The cable sheaths are solidly grounded via bonding leads of 5 μH per phase and the grounding resistance at both cable ends is 1 Ω, as shown in Fig. 2. Parallel to the cable system, a metallic gas/oil coated pipeline is assumed. The pipeline has a separation distance $d = 1$ m from $y = 0$ m for both cable arrangements. The properties of the pipeline are illustrated in Fig. 3.

Table 1
Adjusted cable data.

Parameter	Value
Conductor radius	0.56 cm
Conductor resistivity	$2.42 \cdot 10^{-8}$ Ω•m
Sheath resistivity	$1.02 \cdot 10^{-7}$ Ω•m
Conductor / sheath permeability	1.0
Sheath inner radius	1.33 cm
Sheath outer radius	1.51 cm
Total radius	1.62 cm
Insulation permittivity	2.634
Jacket permittivity	2.5
Insulation / Jacket permeability	1.0

The cable system has a length of $l = 4000$ m. The pipeline is modelled with the same length as the cable system in the part of the parallel routing; the pipeline outside this part is represented by an equivalent impedance equal to its characteristic impedance [17], i.e., 152 Ω, connected at nodes P1 and P2 (Fig. 3). Therefore, the pipeline actually extends for a few kilometres beyond the parallel routing of 4 km without earthing.

For the simulation of the harmonic induced voltages on the cable sheaths and the pipeline, frequency-domain scan is applied by using the exact-pi model of the EMTP-RV software [13]. The per-unit-length parameters, i.e., self and mutual resistance, inductance and capacitance of the cable system and the pipeline, are formulated in the corresponding matrices of order 7 × 7, according to [18]. On this basis, the cable impedances are calculated by taking into account the skin effect and lossy earth, while proximity effect is not included. The effect of lossy earth is represented by means of the impedance earth correction

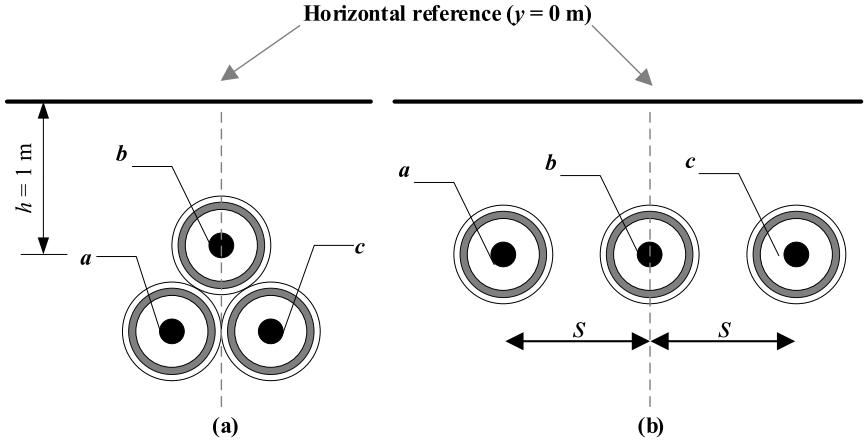

Fig. 1. MV cable in a) trefoil and b) horizontal arrangement.

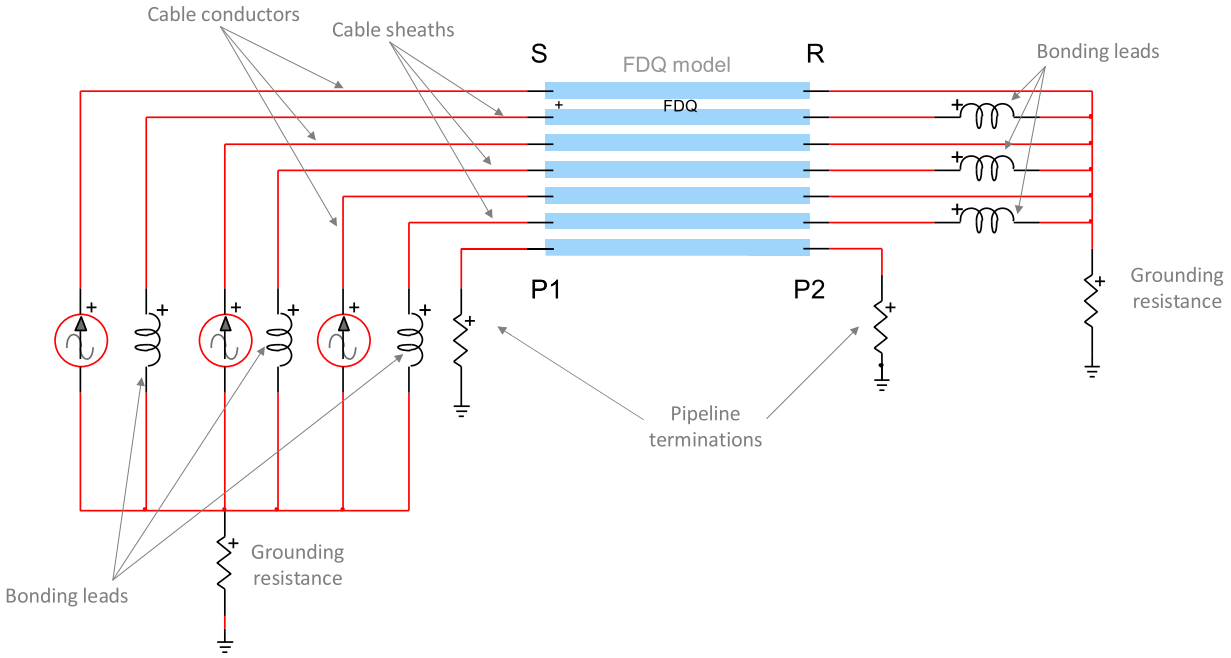

Fig. 2. EMTP-RV simulation model.

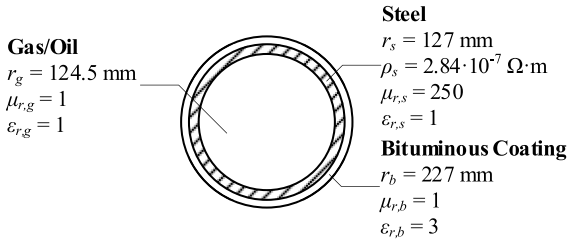

Fig. 3. Geometry and electromagnetic properties of the coated pipeline.

terms proposed by Pollaczek [19], assuming homogeneous earth. In all examined cases, the soil resistivity is equal to 100 Ωm. Nevertheless, since in reality earth is nonhomogeneous, two-layer earth structures can be also considered in the analysis by applying the equivalent homogenous earth resistivity expression of [20]. It should be noted that the influence of the second layer on the harmonic responses is pronounced, due to the increased EM field penetration depth in the examined frequency range; this becomes more evident as the first-to-second soil resistivity ratio increases and the thickness of the first layer decreases [14].

4. Benchmarking analysis

For benchmarking, the harmonic induced voltages at the cable sheaths as well as at the pipeline are simulated using the exact-pi model in EMTP-RV. The main objective of this analysis is to resolve and compare the impact of each harmonic on the induced voltages in a consistent way. The cable system is excited by odd harmonic currents of the 1st (60 Hz) to 15th order, by applying sequentially the corresponding current sources at cable end *S*. Each injected current harmonic has 1 p.u. amplitude in each phase conductor. The phase sequence of the harmonics follows the positive-zero-negative sequence pattern, starting from the 1st and followed by the 3rd, 5th, and so on. Therefore, harmonics of order 1, 7 and 13 are positive-sequence, harmonics of order 3, 9 and 15, i.e., triplen harmonics, are zero-sequence and of order 5 and 11 are negative-sequence. The phase angle displacement of the conductor currents was assumed to be ± 2π/3 rads for nontriplen harmonics and 0 rad for the triplen harmonic frequencies [1].

4.1. Theoretical analysis

To provide in-depth understanding of the influence of individual system components on the harmonic induced voltages, the theoretical background of [17] is adopted. The harmonic induced voltage along a line (*L*) at a distance *x* from its sending end caused by a single power line (*C*) carrying a current I_h of harmonic order *h* can be approximated by [17]:

$$\mathbf{V}_h(x) = \frac{(R_1 + R_2)\cdot\mathbf{z}_h\cdot x - R_1\cdot\mathbf{z}_h\cdot\ell}{R_1 + R_2 + \mathbf{z}_h\cdot\ell}\cdot\left(-\frac{\mathbf{z}_{m-h}}{\mathbf{z}_h}\mathbf{I}_h\right) = \mathbf{K}_h\cdot\mathbf{I}_h \tag{1}$$

where R_1 and R_2 are the grounding resistances at the ends $x = 0$ and $x = \ell$ of line *L*, respectively; $\mathbf{z}_h$ is the per-unit length series impedance of line *L*, $\mathbf{z}_{m-h}$ is the per-unit length mutual impedance between lines *L* and *C*, and ℓ is the total parallel routing length. It is clear from (1) that generally the induced voltage increases with respect to ℓ. In addition, the induced voltage at the ends of line *L* is a function of the corresponding grounding resistance, i.e., at $x = 0$ a function of R_1 and at $x = \ell$ a function of R_2. The total induced voltage $\mathbf{V}_h^{\text{tot}}(x)$ excited by a three-phase system (*a, b, c*) will be given as the vector sum of the resulting voltages $\mathbf{V}_h^a(x)$, $\mathbf{V}_h^b(x)$ and $\mathbf{V}_h^c(x)$ corresponding to each current:

$$\mathbf{V}_h^{\text{tot}}(x) = \mathbf{V}_h^a(x) + \mathbf{V}_h^b(x) + \mathbf{V}_h^c(x). \tag{2}$$

Specifically, the induced voltage for the zero ($\mathbf{V}_h^{\text{tot0}}(x)$), positive ($\mathbf{V}_h^{\text{tot1}}(x)$) and negative ($\mathbf{V}_h^{\text{tot2}}(x)$) sequence harmonics can be described in generic form by (3).

$$\begin{bmatrix}\mathbf{V}_h^{\text{tot0}}(x)\\ \mathbf{V}_h^{\text{tot1}}(x)\\ \mathbf{V}_h^{\text{tot2}}(x)\end{bmatrix} = \mathbf{K}_h^a\begin{bmatrix}I_h^{a0}\angle\varphi_h^{a0}\\ I_h^{a1}\angle\varphi_h^{a1}\\ I_h^{a2}\angle\varphi_h^{a2}\end{bmatrix} + \mathbf{K}_h^b\begin{bmatrix}I_h^{b0}\angle\varphi_h^{a0}\\ I_h^{b1}\angle\varphi_h^{a1} - 2\pi/3\\ I_h^{b2}\angle\varphi_h^{a2} + 2\pi/3\end{bmatrix} + \mathbf{K}_h^c\begin{bmatrix}I_h^{c0}\angle\varphi_h^{a0}\\ I_h^{c1}\angle\varphi_h^{a1} + 2\pi/3\\ I_h^{c2}\angle\varphi_h^{a2} - 2\pi/3\end{bmatrix} \tag{3}$$

where $\mathbf{K}_h^i$ is defined by (1), I_h^{i0}, I_h^{i1}, I_h^{i2} is the amplitude of the zero, positive and negative harmonic currents, and *i* corresponds to *a, b*, or *c*. Note that the phase angle of the zero, positive and negative harmonic currents of phase *b* and *c* is related to the corresponding of phase *a*, i.e.,

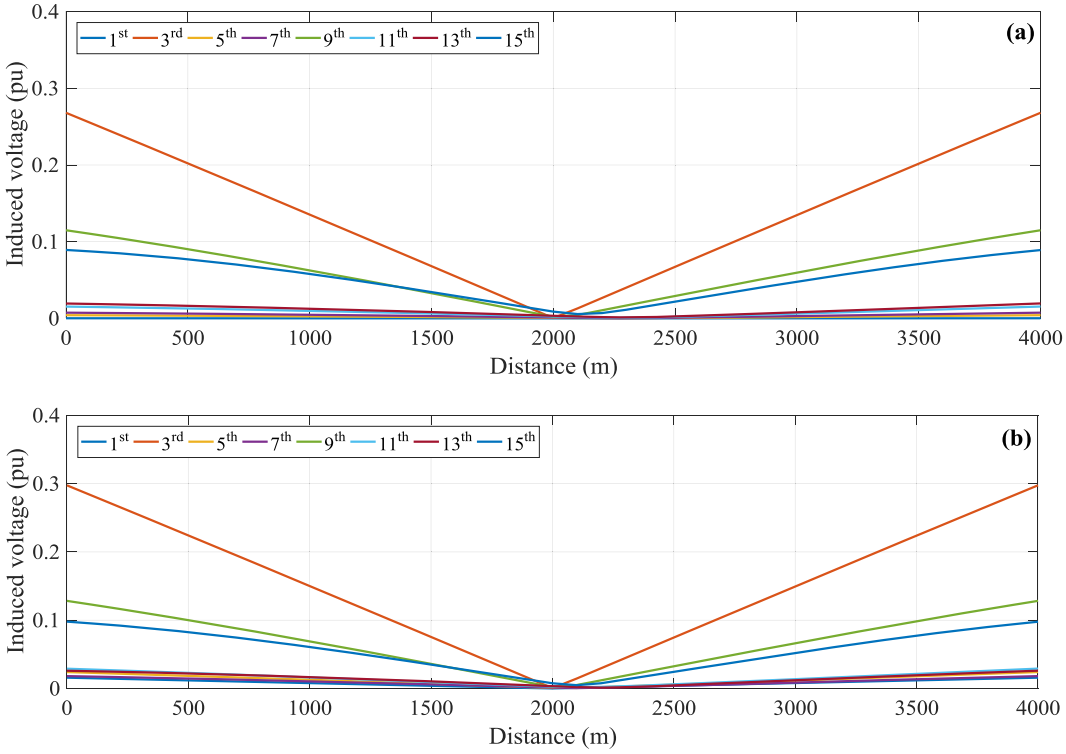

Fig. 4. Harmonic induced voltage profiles along cable sheath a for the a) trefoil and b) horizontal arrangements.

$\varphi_h^{a_0}$, $\varphi_h^{a_1}$, $\varphi_h^{a_2}$.

4.2. Simulation of induced voltages

The profiles of the harmonic induced voltages of the cable sheath at phase a and of the pipeline for both cable arrangements are presented in Figs. 4 and 5, respectively. Note that, in this case, 40 exact-pi equivalents of 100-m are used in cascaded connection. The induced voltages at the two ends for all harmonics present a phase angle shift of 180°, as results also from (1)-(3), assuming $R_1 = R_2$, $x = 0$ and $x = \ell$. Due to this phase angle shift, the harmonic voltage profiles along the sheath as well as along the pipeline acquire maximum values at the ends, while in the middle, i.e., at $x = \ell/2 = 2000$ m, become zero. The lower harmonic voltages at the cable sheath compared to that of the

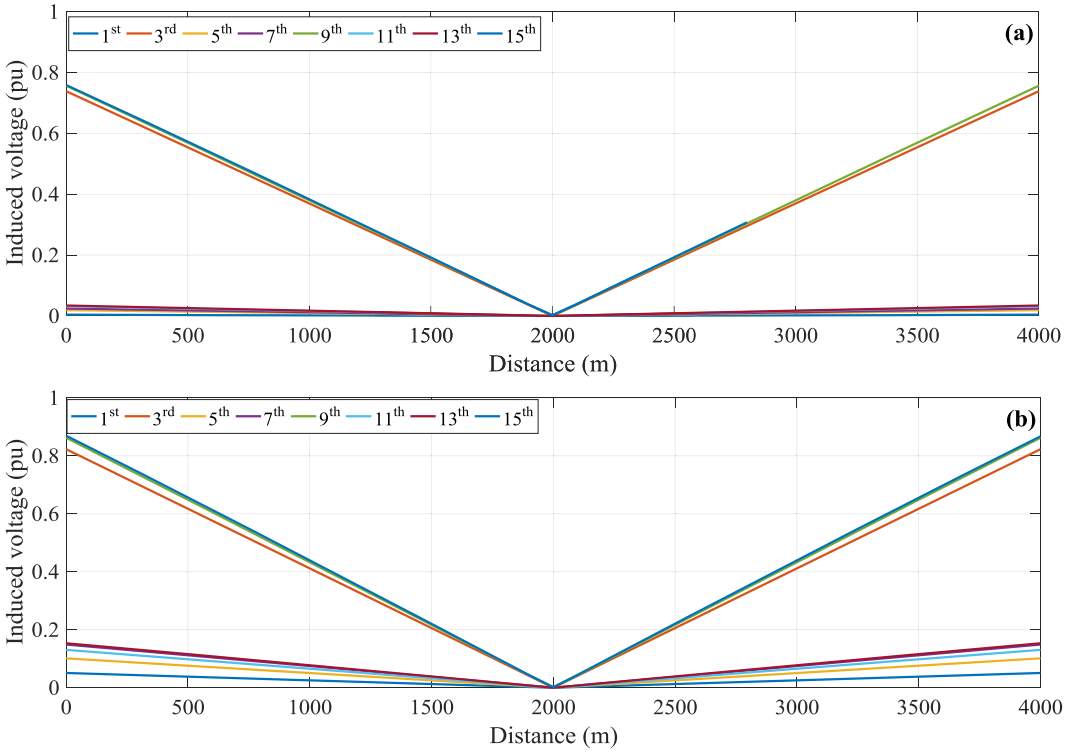

Fig. 5. Harmonic induced voltage profiles along the pipeline for the a) trefoil and b) horizontal arrangements.

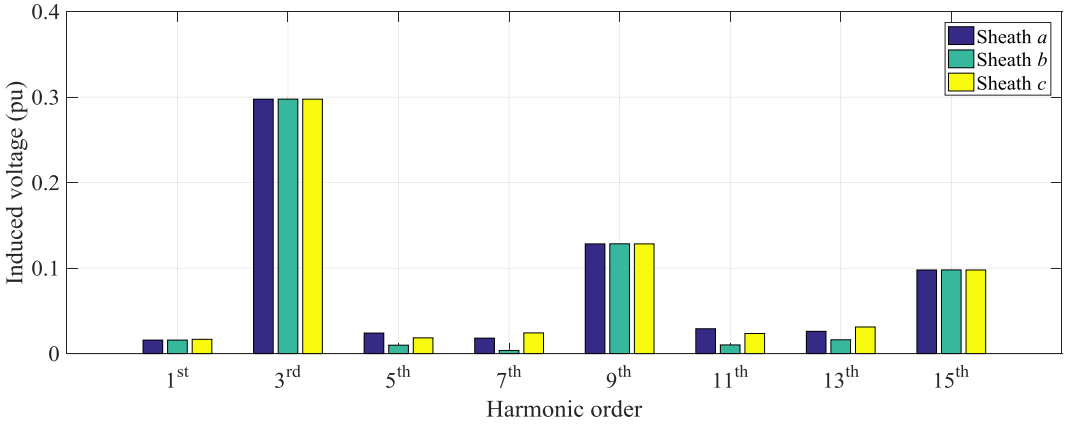

Fig. 6. Harmonic induced voltages at the end R of cable sheaths for the horizontal cable arrangement.

pipeline are mainly due to the lower value of the grounding resistance, since the pipeline is terminated at 152 Ω.

In Fig. 6, the harmonic induced voltages at the end *R* of the cable sheaths of the horizontal cable arrangement are summarized by means of a bar chart. It is shown that for the nontriplen harmonics the sheath voltages at each phase differ slightly; moreover, the phase where the highest value is observed, differs with the harmonic order. For the positive- and negative-sequence harmonics the highest values are obtained at phase *c*, and *a*, respectively. For the triplen harmonics, similar sheath voltage levels are observed at all phases. The induced sheath voltages for the trefoil arrangement are similar at all cable phases, thus results only for phase *a* are presented.

The influence of the harmonic order on the voltages at end *R* of the cable sheath at phase *a* is examined in Fig. 7, considering both the horizontal and the trefoil cable arrangements. Similar investigations are also carried out for the pipeline voltages at the end P2, in Fig. 8.

Starting from Fig. 8, results reveal that for both cable arrangements the harmonic induced voltages of the same sequence increase slightly with the harmonic order by means of the Faraday law. For example, for the triplen harmonics, the induced sheath voltage of the 15th harmonic acquires the highest values followed by the 9th and finally by the 3rd. Regarding the calculated voltage levels, it is evident that high harmonic induced voltages are obtained for the triplen harmonics exceeding significantly the voltage levels excited by the nontriplen harmonics. For the zero-sequence triplen harmonics, the total harmonic induced voltage of (3) is almost the algebraic sum of $\mathbf{V}^a$, $\mathbf{V}^b$ and $\mathbf{V}^c$. Note that, in fact, the electromagnetic field excited by each cable phase is the result of the injected current in the conductor taking also into account the effect of partial cancelling from the corresponding sheath current. The triplen harmonic sheath currents and consequently the corresponding sheath voltages in Fig. 7 are the result of inductive coupling (causing circulating currents) and of the returning zero-sequence currents; the effect of the latter becomes predominant as the sheath grounding increases (see also Section 5.3). Therefore, in Fig. 7, as the resistance of the cable sheath increases with frequency, the level of the triplen harmonic sheath currents reduces, resulting consequently into lower sheath voltages (see. Eq. (3)).

The induced nontriplen harmonic voltages on the pipeline can be analysed taking into account the fact that the pipeline is located at a distant point away from the cable system, i.e., the excitation source. The resulting induced voltage is almost eliminated by means of the vector sum of the total flux density, as described by (3). In particular, from Fig. 8 it can be realized that in the horizontal cable arrangement the induced pipeline voltages of all harmonics are higher to those of the trefoil case. This is attributed to the geometric asymmetry in the horizontal arrangement, resulting into different mutual couplings between the pipeline and each current carrying conductor; thus, consequently to higher magnetic field level and induced voltage. Similar remarks regarding the nontriplen harmonics also apply for the induced voltages at the cable sheaths, as shown in Fig. 7.

In summary, it can be concluded that the most pronounced harmonic induced voltages both at the cable sheaths and the pipeline are observed for the 3rd harmonic and its odd multiples.

4.3. Comparison of simulation models

The exact-pi model is used for the accurate calculation of the induced voltages in cable configurations, since the model results are based on the exact solution of the distributed parameter transmission line equations [15]. Additionally, the accuracy of the nominal-pi of

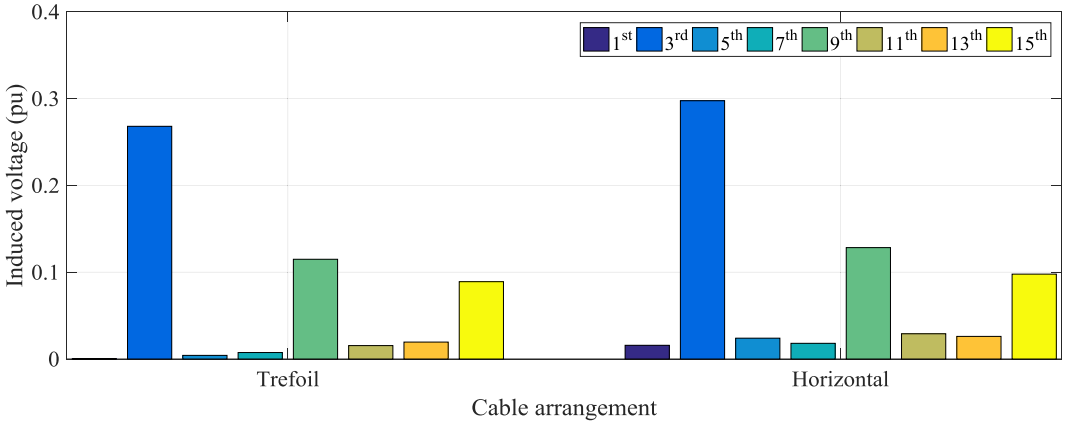

Fig. 7. Harmonic induced voltages at the end R of cable sheath a for both cable arrangements.

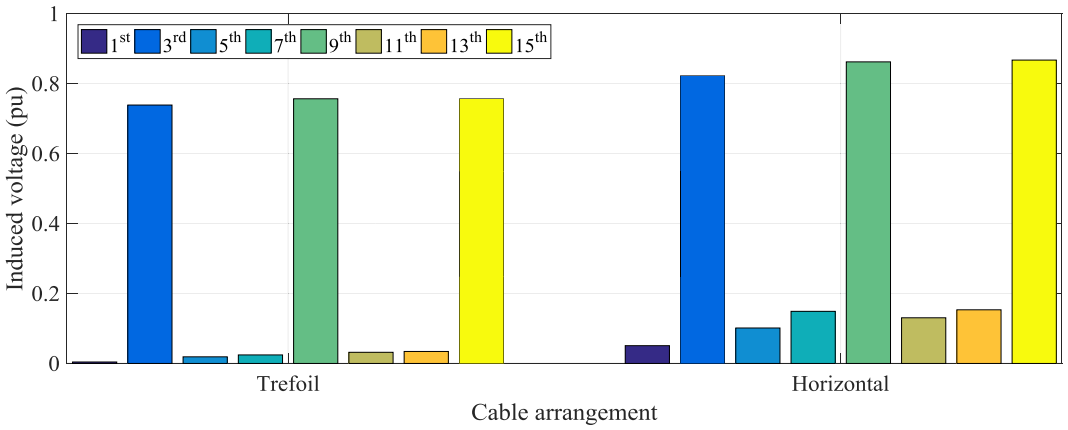

Fig. 8. Harmonic induced voltages at the end P2 of the pipeline for both cable arrangements.

ATP-EMTP [21] and the wideband (WB) of EMTP-RV software [22] cable models is also evaluated. The nominal-pi is a simplification of the exact-pi and can be used for the analysis of electrically short cables, i.e., at low frequencies and short lengths [15]. Therefore, the nominal-pi is widely adopted for the investigation of EMI problems by means of circuit analysis. Although the examined problem refers to steady-state, the WB model is also examined since it can be used in time-domain simulations of harmonic distorted voltage and current waveforms. The WB model uses complex poles and zeros for the rational approximation of the frequency-dependent phase-domain characteristic admittance and wave propagation matrices; it also takes into account the frequency dependence of the modal transformation matrix. Thus, it can be considered as the most accurate time-domain model, especially for underground cable systems modeling [15]. In all simulations, the fitting process of the relevant WB transfer functions is performed in the frequency range from 0.01 Hz to 10 MHz using 50 poles and convergence tolerance 0.01%. Finally, Finite Element Method (FEM) in COMSOL Multiphysics® Modeling Software [23] is also employed. The inductive mechanism is studied by means of the modeling presented in [24]. In particular, the inductive coupling is formulated in a 2D plane configuration by solving Maxwell's equations for magnetic field and induced current distributions in and around conductors. The derivation of current and voltage profiles requires the solution of this problem for different out-of-plane thicknesses in terms of a parametric study, realizing an actual 2.5D simulation. In addition, the extended capability of simulating unbalanced currents is implemented by proper circuit connections at each cable end, satisfying Kirchhoff's laws.

The relative difference defined in (4) is calculated for the results obtained by the WB, the nominal-pi models and FEM approach, assuming the exact-pi as reference:

$$diff\,(\%) = |V_{WB/nominal-pi} - V_{exact-pi}|/V_{exact-pi}. \quad (4)$$

In Figs. 9 and 10 the resulting relative differences of the calculated induced voltages of the cable sheath at phase *a* and at the pipeline are compared, respectively. From Fig. 9, it is shown that the nominal-pi model and the WB match very accurately the exact-pi solution for all harmonics. This is more evident for the induced sheath voltages, since differences are lower than 2.5% in all cases. Regarding the induced harmonic voltages at the pipeline, for the nominal-pi model, differences increase slightly with the harmonic order. By analysing the results obtained by the WB model, differences are observed only at specific frequencies, though they do not surpass 8.8%; the differences are mainly attributed to the error introduced in the fitting of the WB transfer function. Therefore, it can be generally concluded that both the WB and the nominal-pi models can be used for the accurate calculation of the harmonic induced voltages on cable sheaths and pipelines for the examined frequency range and for cable lengths up to 4 km.

Regarding FEM results for the horizontal cable arrangement, negligible differences are observed for all harmonics. Small differences are also obtained for the triplen harmonics results (lower than 2%) for the trefoil arrangement. However, in the trefoil arrangement, increasing differences with frequency (may slightly exceed 10%) are calculated for the nontriplen harmonic voltages. This is attributed to the influence of eddy currents in the sheaths [1] as well as to proximity effect. The effect of eddy currents becomes more important for nontriplen harmonics [1], whereas proximity effect is evident in the trefoil case. However, nontriplen harmonic voltage levels are generally low (less than 0.02 p.u.), thus not of major importance in the calculation of the harmonic induced voltages. Therefore, from the above remarks it can be generally concluded that the accuracy of the exact-pi, the nominal-pi and the WB models is verified.

5. Results with measured data

To investigate the impact of harmonics on the induced voltages on the cable sheaths and the pipeline, considering measured harmonic currents, the data of Table 2 are used. These are based on field measurements in 14.4 kV and 25 kV feeders [2]. In this case, the current harmonic magnitudes are significantly lower compared to the fundamental at 60 Hz. Simulations are performed using the exact-pi model.

In Fig. 11, the harmonic induced voltages at the cable sheath *a* and the pipeline are compared for the two cable arrangements for $\ell = 4000$ m. The induced sheath voltages of the nontriplen harmonics are almost eliminated in the trefoil arrangement. On the contrary, the 3rd harmonic acquires high levels, exceeding that of the fundamental at 60 Hz. For the horizontal arrangement, the induced sheath voltages of the triplen harmonics are close to the corresponding of the trefoil arrangement, as shown in the previous section. However, higher induced voltages are observed for the nontriplen harmonic components compared to the trefoil cable arrangement. These are mainly due to the geometry asymmetry of the horizontal arrangement. Similar remarks are also drawn from Fig. 11b for the harmonic induced voltage at the pipeline end. Comparable induced voltage levels are observed for the 9th harmonic for both cable arrangements; in particular, for the trefoil arrangement, the 9th harmonic induced voltage exceeds even that of the fundamental.

5.1. Influence of pipeline separation distance

The influence of the horizontal separation distance *y* is investigated on the harmonic induced voltages at the pipeline ends P1 and P2. The separation distance between the examined cable system and the pipeline is assumed varying, from 1 m to 50 m, with the latter being the maximum interference limit according to [25]. Fig. 12 demonstrates the

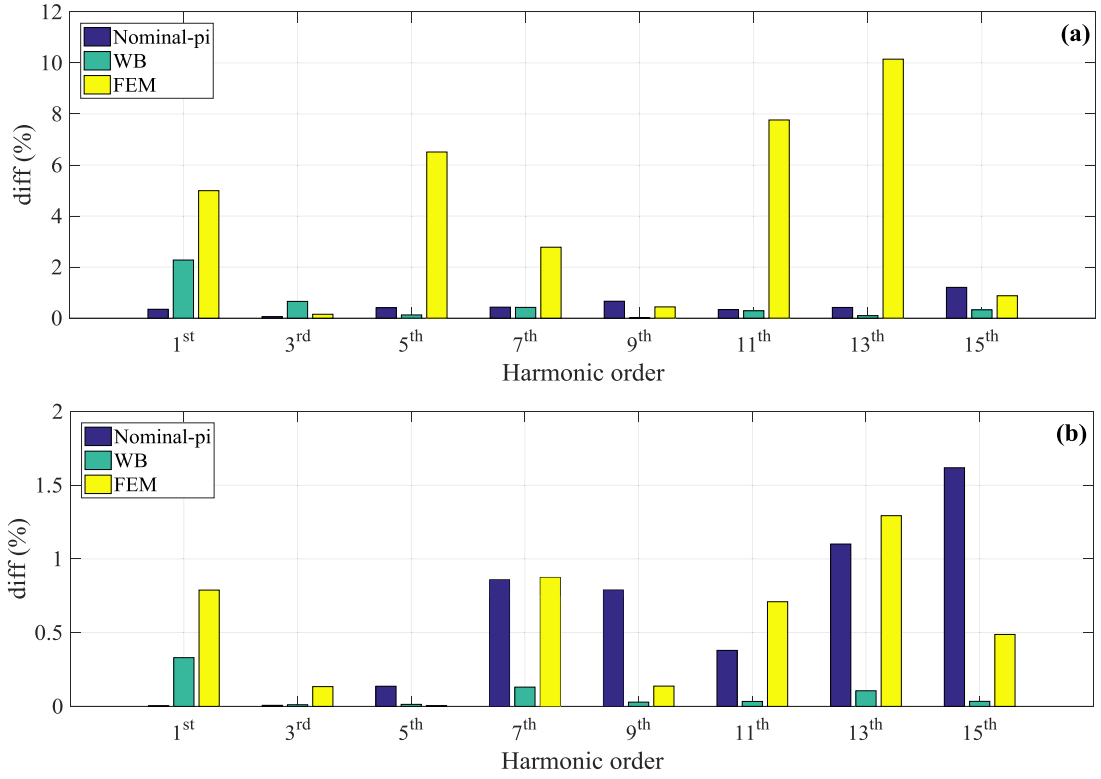

Fig. 9. Comparison of the harmonic induced voltages at the end R of cable sheath a for a) trefoil and b) horizontal cable arrangements.

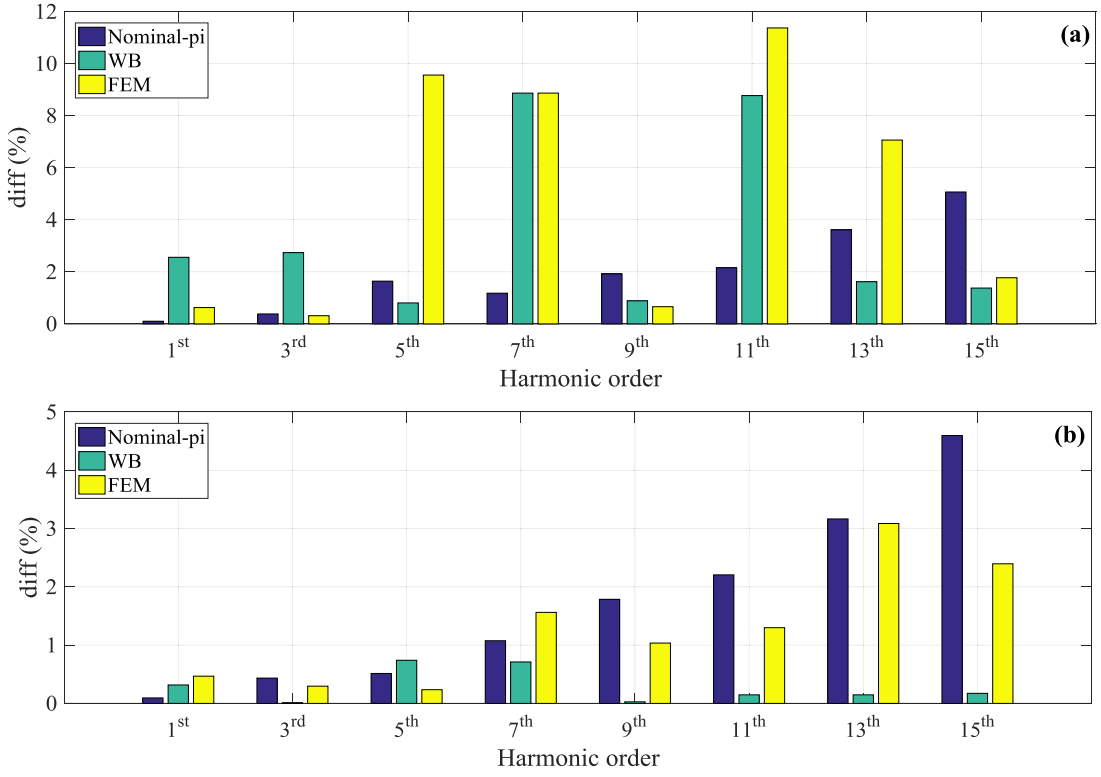

Fig. 10. Comparison of the harmonic induced voltages at the end P2 of the pipeline for a) trefoil and b) horizontal cable arrangements.

Table 2
Average harmonic sequence currents.

Harmonic order	Sequence	Normalized value (p.u.)
1st	Positive	1.000
3rd	Zero	0.070
5th	Negative	0.052
7th	Positive	0.022
9th	Zero	0.016
11th	Negative	0.006
13th	Positive	0.003
15th	Zero	0.002

variation of the induced harmonic voltages at end P2 for the trefoil and the horizontal arrangements. Similar results are also obtained for node P1.

Generally, the induced harmonic voltage levels are reduced and are practically eliminated, as y increases. In fact, the influence of y on the induced voltages can be directly realized from (1); as y increases, $z_{m\text{-}h}$ decreases, and evidently reduced voltages levels are obtained. In particular, as y increases, the effect of the induced voltages of the triplen harmonics becomes more important compared to that of the fundamental at 60 Hz. This is more evident for the 3rd harmonic, which is predominant and results in induced voltage levels over 0.02 p.u. for all examined y values and for both cable arrangements. In the trefoil arrangement, the 3rd and the 9th harmonic induced voltage levels at $y = 50$ m are higher compared to the fundamental at $y = 1$ m. In the horizontal arrangement, the induced voltage level of the 9th harmonic is significantly lower to that of the fundamental at $y = 1$ m. However, as y increases, comparable voltage levels between the fundamental and the 9th harmonic are deduced.

5.2. Influence of soil resistivity

Next, the influence of soil resistivity on the harmonic induced voltages is examined. As shown in Fig. 13 for the horizontal cable arrangement, the calculated induced sheath voltages of all harmonics are slightly affected by the soil resistivity. Similar remarks can be also concluded for the trefoil arrangement; thus, results are not presented.

In Fig. 14, the harmonic induced voltages at the pipeline end P2 are illustrated for both cable arrangements. Only the harmonic induced voltages of the fundamental (used as reference) and of triplen harmonics are presented. Since triplen harmonics are zero-sequence, they are the mostly affected harmonics. As shown, the level of the induced voltages of the triplen harmonics increases slightly with soil resistivity for both cable arrangements. In general, the effect of earth conduction effects would be more significant with the asymmetry of the injected currents.

5.3. Influence of grounding resistance

As already mentioned, a very important parameter of the problem is the cable sheath grounding resistance. Fig. 15 shows the effect of the grounding resistance on the harmonic sheath and pipeline voltages. Also in this case the harmonic induced voltages of the fundamental and the triplen harmonics are presented. It is evident that, by increasing the grounding resistance at both cable ends, the harmonic sheath voltage increases accordingly. This, however, results in increasing returning currents through the sheaths and consequently to higher cancelling of the electromagnetic field excited by the injected currents in the cable conductors. Therefore, from Figs. 15b and 15d, it can be realized that the harmonic induced voltage levels of all harmonics at the pipeline reduce as the grounding resistance increases.

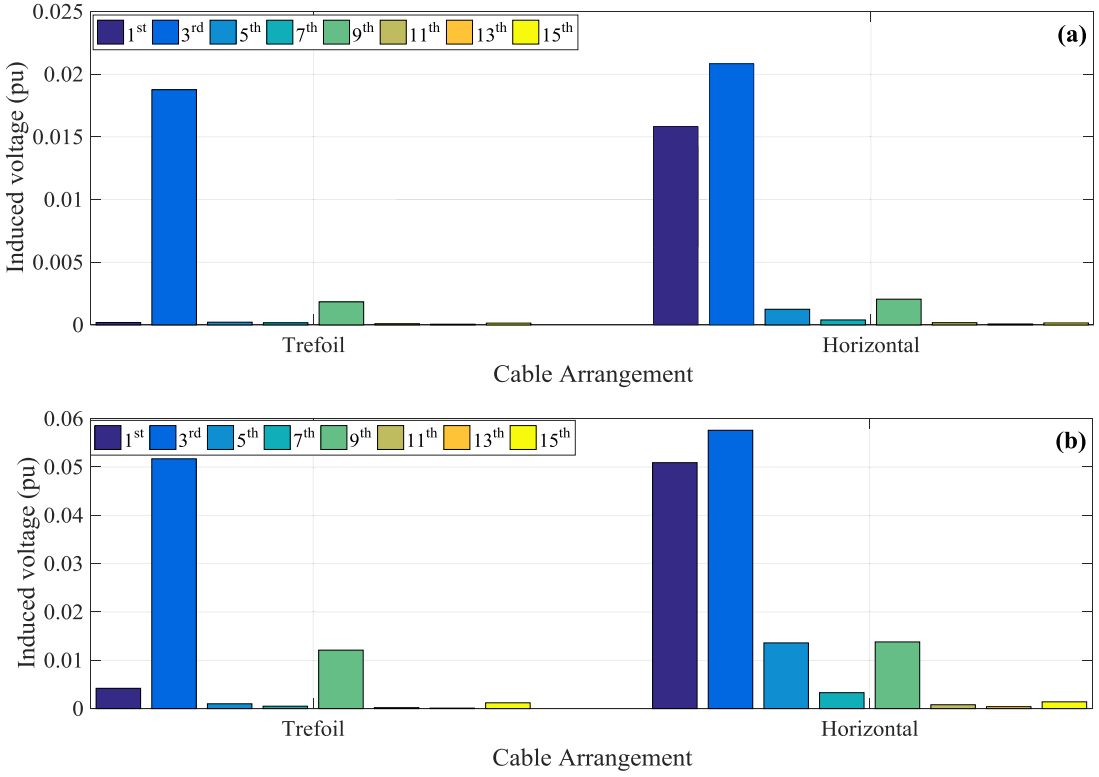

Fig. 11. Harmonic induced voltage levels at a) end R of cable sheath a and b) at end P2 of the pipeline. Both cable arrangements.

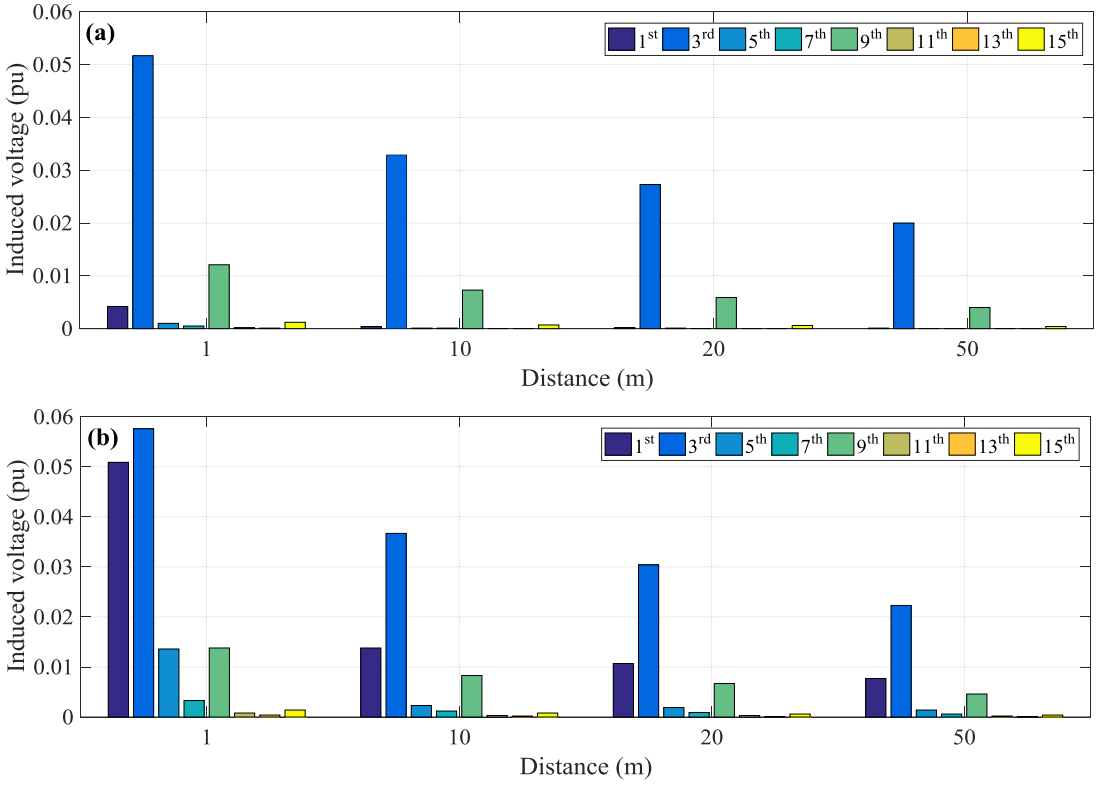

Fig. 12. Influence of distance on the harmonic induced voltage levels at end P2 of the pipeline for the a) trefoil and b) horizontal cable arrangements.

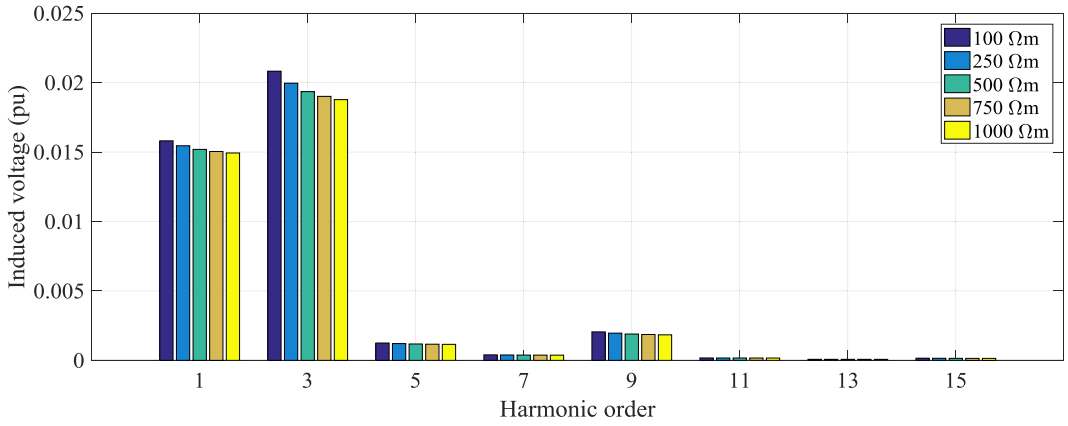

Fig. 13. Influence of soil resistivity on the harmonic induced voltage levels at end R of the cable sheath a. Horizontal cable arrangement.

6. Time-domain simulations

The final set of simulations pertain to calculating the time-domain waveforms of the induced voltages on the cable sheaths and the pipeline. The results have been obtained by using the WB cable model of EMTP-RV, assuming the same conditions and parameters for both cable arrangements, as in Section 4. Two operating conditions are taken into account. In the first, the measured harmonic currents of [2] are used, assuming that the harmonic injected currents in each cable conductor are of the same magnitude (as in Table 2); this corresponds to a 'balanced' operating condition. In the second case the data of [2] are used again, but taking also into account the current asymmetry, as originally recorded and presented [2]. This operating condition is characterized as 'unbalanced'. Additionally, in order to simulate accurately the simultaneous effect of all harmonics on the induced voltages, measured current phase angles of each harmonic are also assumed, based on the field measurements of [11]. In Fig. 16, the inducing current waveforms of the three cable conductors are depicted for the two operating conditions. The magnitude of all injected harmonic currents has been reduced with respect to the rated cable current at 60 Hz, i.e., 380 A.

In Fig. 17, the induced cable sheath and pipeline harmonic voltages are illustrated. For both the cable sheath and the pipeline waveforms, highly distorted non-sinusoidal periodic patterns are calculated. As expected, this becomes more evident in the unbalanced case, due to the asymmetry in the current waveforms, where higher peak voltages are observed compared to the balanced operating condition. Moreover, it

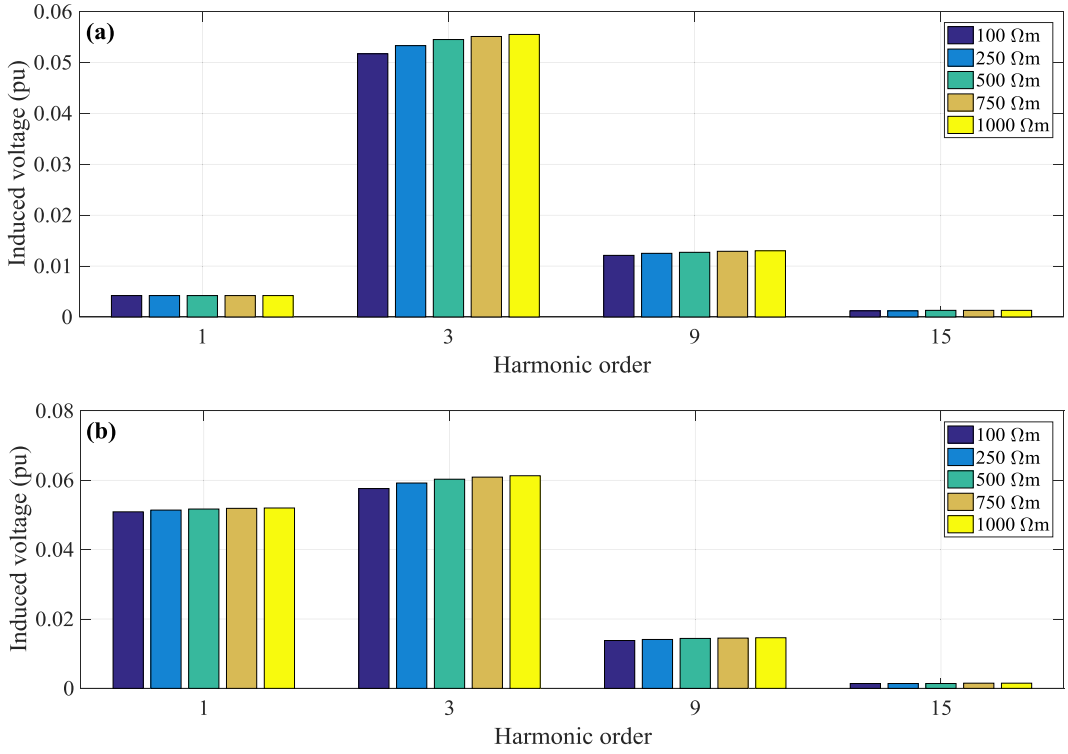

Fig. 14. Influence of soil resistivity on the harmonic induced voltage at end P2 of the pipeline for the a) trefoil and b) horizontal cable arrangements.

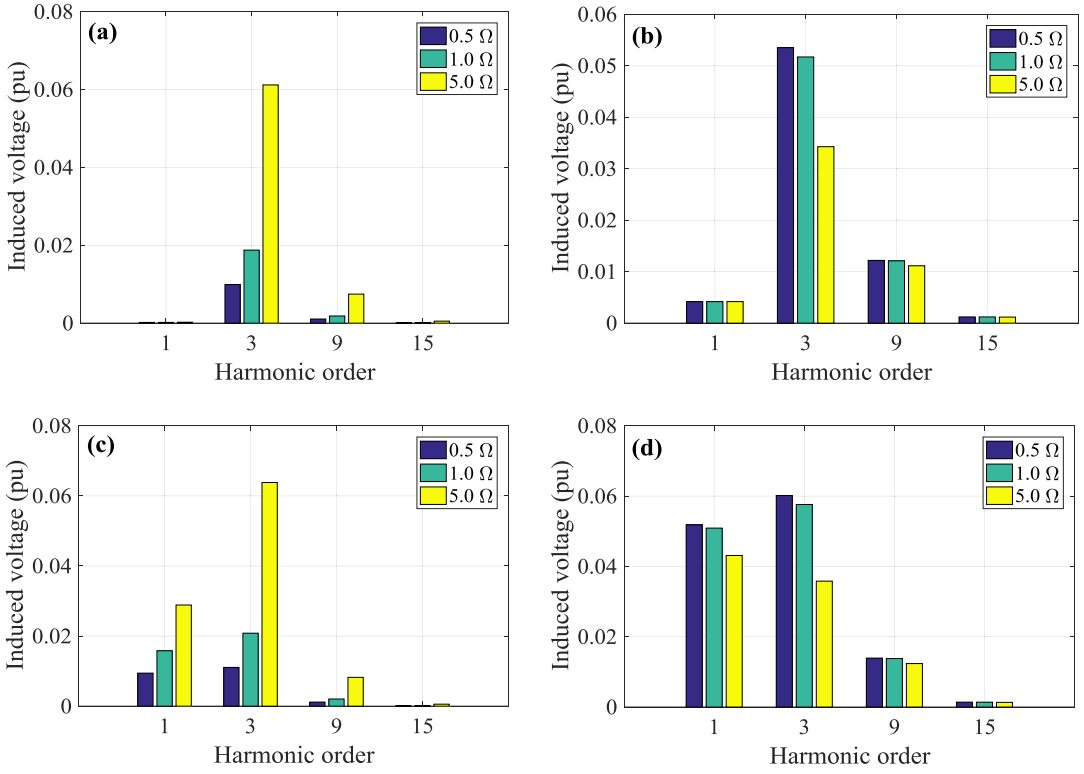

Fig. 15. Influence of grounding resistance. Harmonic voltages for the trefoil arrangement at a) end R of the cable sheath a and b) end P2 of the pipeline; for the horizontal arrangement at c) end R of the cable sheath a and d) end P2 of the pipeline.

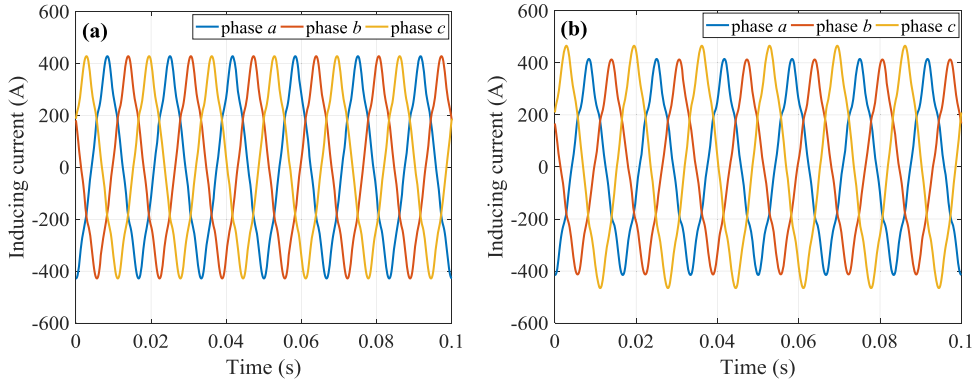

Fig. 16. Harmonic inducing current waveforms of the three cable conductors for the a) balanced and b) unbalanced operating conditions.

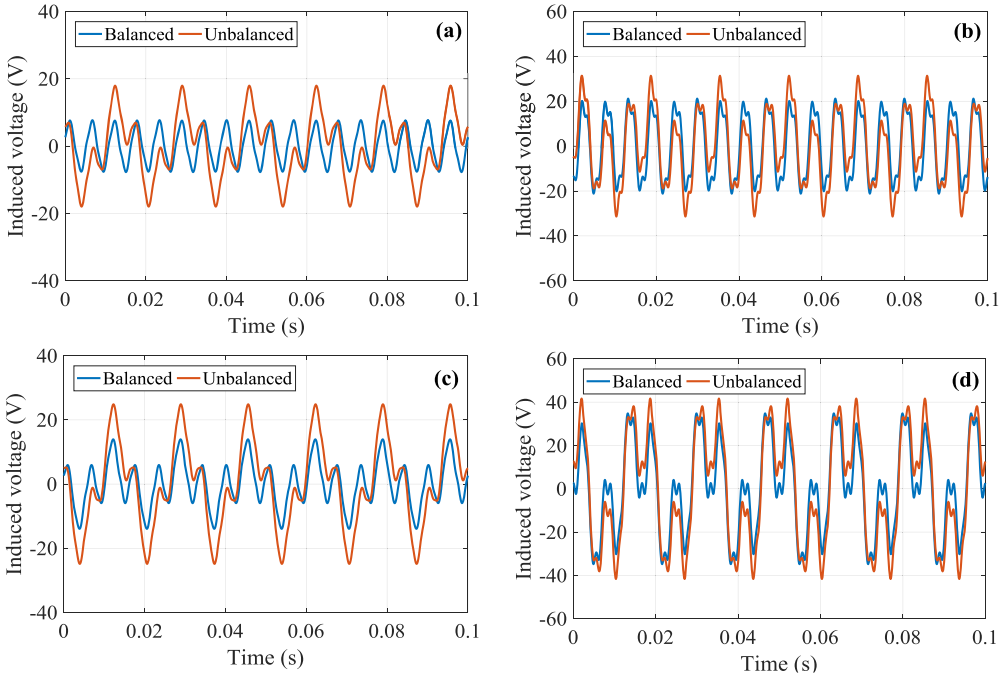

Fig. 17. Harmonic voltage waveforms for the trefoil arrangement at a) end R of the cable sheath a and b) end P2 of the pipeline; for the horizontal arrangement at c) end R of the cable sheath a and d) end P2 of the pipeline.

can be concluded that the effect of the current asymmetry is more evident on the cable sheath voltages compared to that of the pipeline, since significant divergences between the voltage waveform patterns of the two operating conditions are observed.

7. Conclusions

Harmonic induced voltages on cable sheaths and pipelines excited by MV underground cables systems were investigated using simulation software. From the conducted analysis, the main findings are summarized as follows:

- Induced cable sheath and pipeline voltages caused by triplen harmonics can be significantly higher than the induced voltages of the fundamental frequency at 60 Hz. This might be also evident in cases of large separation distances between the cables and the pipeline, e.g. 50 m.
- Harmonic induced voltages are higher in the horizontal cable arrangement compared to the trefoil. In general, harmonic voltages at the cable sheaths and at the pipeline increase with the asymmetry in the cable system, both in terms of the configuration geometry as well as of current unbalance.
- Other cable formations, such as the touching horizontal (flat) or spaced trefoil formation, can be also realised and examined by properly adjusting the cable spacing *s*. Results are expected to slightly differ, since they are mainly affected by the current rating of each case study and the cable system asymmetry.
- The nominal-pi and the wideband simulation models perform very accurately in all examined cases, compared to the exact-pi. Comparisons with the FEM approach verified the validity of the above simulation models. For higher accuracy, especially regarding nontriplen calculations, the influence of eddy currents and of the proximity effect should be considered.
- The cable sheath grounding resistance is of major importance for the analysis of the problem; this parameter determines the level of returning currents through the sheaths and consequently the total electromagnetic field excited by the cable system.
- The soil resistivity affects slightly the harmonic induced voltages in case of triplen harmonics. In the case of nontriplen harmonics, the effect of earth conduction is negligible.

It can be generally concluded that the impact of harmonics excited by cable distribution systems on EMI should be examined in relevant studies and included in future versions of the corresponding standards and recommendations.

CRediT authorship contribution statement

T.A. Papadopoulos: Conceptualization, Methodology, Investigation, Formal analysis, Writing - original draft. **I.P. Chaleplidis:** Investigation, Formal analysis, Software. **A.I. Chrysochos:** Methodology, Software, Validation, Writing - review & editing. **G.K. Papagiannis:** Supervision. **K. Pavlou:** Supervision.

Declaration of Competing interest

The authors declare that they have no known competing financial interests or personal relationships that could have appeared to influence the work reported in this paper.

The authors declare the following financial interests/personal relationships which may be considered as potential competing interests:

Acknowledgement

The Power Systems Laboratory of Democritus University of Thrace is an EMTP-RV official educational partner and would like to thank POWERSYS SOLUTIONS for offering the academic license. The authors would like also to thank Dr. I. Kocar for details regarding distribution cables in Canada and U.S.A.

References

[1] C. Demoulias, D.P. Labridis, P.S. Dokopoulos, K. Gouramanis, Ampacity of Low-Voltage Power Cables Under Nonsinusoidal Currents, IEEE Trans. Power Del. 22 (1) (2007) 584–594.
[2] J. Yong, B. Xia, H. Yong, W. Xu, A.B. Nassif, T.C. Hartman, Harmonic Voltage Induction on Pipelines: measurement Results and Methods of Assessment, IEEE Trans. Power Del. 33 (5) (2018) 2170–2179.
[3] C.G. Kaloudas, T.A. Papadopoulos, K.V. Gouramanis, K. Stasinos, G.K. Papagiannis, Methodology for the selection of long-medium voltage power cable configurations, IET Gener., Trans. & Distrib. 7 (5) (2013) 526–536.
[4] CIGRE Working Group 36.02, "Guide Concerning Influence of High Voltage AC Power Systems on Metallic Pipelines," 1995.
[5] F.P. Dawalibi, R.D. Southey, Analysis of Electrical Interference from Power Lines to Gas Pipelines Part I: computation Methods, IEEE Trans. Power Del. 4 (3) (1989) 1840–1846.
[6] G.C. Christoforidis, D.P. Labridis, P.S. Dokopoulos, Inductive Interference on Pipelines Buried in Multilayer Soil, due to Magnetic Field from Nearby Faulted Power Lines, IEEE Trans. EMC 47 (2) (2005) 254–262.
[7] A. Ametani, R. Baba, T. Umemura, Y. Hosokawa, Induced Voltages on a Pipeline due to Electro-Magnetic and Static Coupling with a Power Line, International Conference on Electrical Engineering (ICEE), HongKong, 2007.
[8] T.A. Papadopoulos, G.C. Christoforidis, D.D. Micu, L.L. Czumbil, Medium-voltage cable inductive coupling to metallic pipelines: a comprehensive study, 2014 49th International Universities Power Engineering Conference (UPEC), Cluj-Napoca, 2017.
[9] J. Arrillaga, T.J. Densem, J. Harker, Zero Sequence Harmonic Current Generation in Transmission Lines Connected to Large Convertor Plant, IEEE Trans. Power App. Syst. 102 (7) (1983) 2357–2363.
[10] H. Ding, Y. Zhang, A.M. Gole, D.A. Woodford, M.X. Han, X.N. Xiao, Analysis of Coupling Effects on Overhead VSC-HVDC Transmission Lines from AC Lines with Shared Right of Way, IEEE Trans. Power Del. 25 (4) (2010) 2976–2986.
[11] Y. Wang, J. Yong, Y. Sun, W. Xu, D. Wong, Characteristics of Harmonic Distortions in Residential Distribution Systems, IEEE Trans. Power Del. 32 (3) (2017) 1495–1504.
[12] C.A. Charalambous, A. Demetriou, A. Lazari, A. Nikolaidis, Effects of Electromagnetic Interference on Underground Pipelines caused by the Operation of High Voltage A.C. Traction Systems: the Impact of Harmonics, IEEE Trans. Power Del. 33 (6) (2018) 2664–2672.
[13] J. Mahseredjian, S. Dennetiere, L. Dube, B. Khodabakhchian, L. Gerin-Lajoie, On a new approach for the simulation of transients in power systems, Electr. Power Syst. Res. 77 (11) (2007) 1514–1520.
[14] T.A. Papadopoulos, A.I. Chrysochos, G.K. Papagiannis, Analytical study of the frequency-dependent earth conduction effects on underground power cables, IET Gener., Trans. & Distrib. 7 (3) (2013) 276–287.
[15] T.A. Papadopoulos, A.I. Chrysochos, D.I. Doukas, G.K. Papagiannis, D.P. Labridis, Induced voltages and currents: overview and evaluation of simulation models and methodologies, MedPower16 Conference, Belgrade,Serbia, 2016 November 6-9.
[16] B. Gustavsen, J.A. Martinez, D. Durbak, Parameter determination for modeling system transients – Part II: insulated cables, IEEE Trans. Power Del. 20 (3) (2005) 2045–2050.
[17] A. Ametani, Four-terminal parameter formulation of solving induced voltages and currents on a pipeline system, IET Science, Meas. & Techn. 2 (2) (2008) 76–87.
[18] A. Ametani, A general formulation of impedance and admittance of cables, IEEE Trans. Power App. Syst. 99 (3) (1980) 902–910.
[19] F. Pollaczek, Über das Feld einer unendlich langen wechselstromdurchflossenen Einfachleitung, Elektr. Nachr. Technik 3 (4) (1926) 339–359.
[20] D.A. Tsiamitros, G.K. Papagiannis, P.S. Dokopoulos, Homogenous Earth Approximation of Two-Layer Earth Structures: an Equivalent Resistivity Approach, IEEE Trans. Power Delivery 22 (1) (2007) 658–666.
[21] H.W. Dommel, EMTP Theory Book, Bonneville Power Administration, 1982.
[22] A. Morched, B. Gustavsen, M. Tartibi, A universal model for accurate calculation of electromagnetic transients on overhead lines and underground cables, IEEE Trans. Power Del. 14 (3) (1999) 1032–1038.
[23] COMSOL Multiphysics®, www.comsol.com. COMSOL AB, Stockholm, "COMSOL Multiphysics®, www.comsol.com, COMSOL AB, Stockholm, Sweden".
[24] A.I. Chrysochos, K. Alexandrou, D. Chatzipetros, D. Kossyvakis, G.J. Anders, K. Pavlou, K. Tastavridis, G. Georgallis, Capacitive and Inductive Coupling in Cable Systems – Comparative Study between Calculation Methods, Proceedings of the 10th JICABLE 2019, Paris,France, 2019 June 23 – 27.
[25] EN 50443:2011: Effects of electromagnetic interference on pipelines caused by high voltage a.c. electric traction systems and/or high voltage a.c. power supply systems.